Supplementary information: A lithiophilic TiN-carbon scaffold for lithium-metal anodes, with SEI ionic conductivity boosted by Li_3N formation

Junren Wang, Huaxin Cao, Nikolay Zhelev, Andrea E. Russell, Andrew L. Hector*

School of Chemistry and Chemical Engineering, University of Southampton, SO17 1BJ, UK.
A.L.Hector@soton.ac.uk

This file includes supplementary text, Figs. S1 to S21 and Tables S1 and S2

Supplementary Text

The mass loading of the TiN components in the composites were calculated by thermogravimetric analysis (Figure S2 and Equation S1). The sample mass at 200 °C was taken as the reference mass because up to this temperature the mass loss corresponded to elimination of water and the mass stayed the same between the 100 and 200 °C. Upon heating up to 700 °C, as shown in Figure S2, the TiN@C composite shows a slight weight gain at around 450 °C, which is attributed to the oxidation of TiN. The specific mass ratio of TiN in the composites was calculated as shown in Equation S1, where mass of the composite is "a" gram, and the mass ratio of TiN in the composite is "x". The amount of TiO_2 formed is 79.86ax/59.89 after heating at 700 °C, hence the original loading can be calculated.

$$TiN + 2O_2 \rightarrow TiO_2 + NO_2 \qquad \text{(Equation S1)}$$

$$\frac{61.88}{ax} = \frac{79.86}{79.86ax/61.88}$$

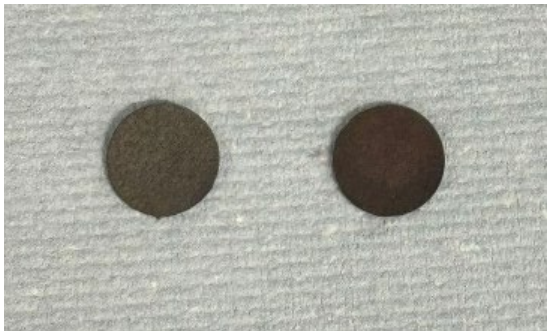

Fig. S1. Photos of self-standing C (left) and TiN@C electrodes (right). Electrodes are 11 mm diameter.

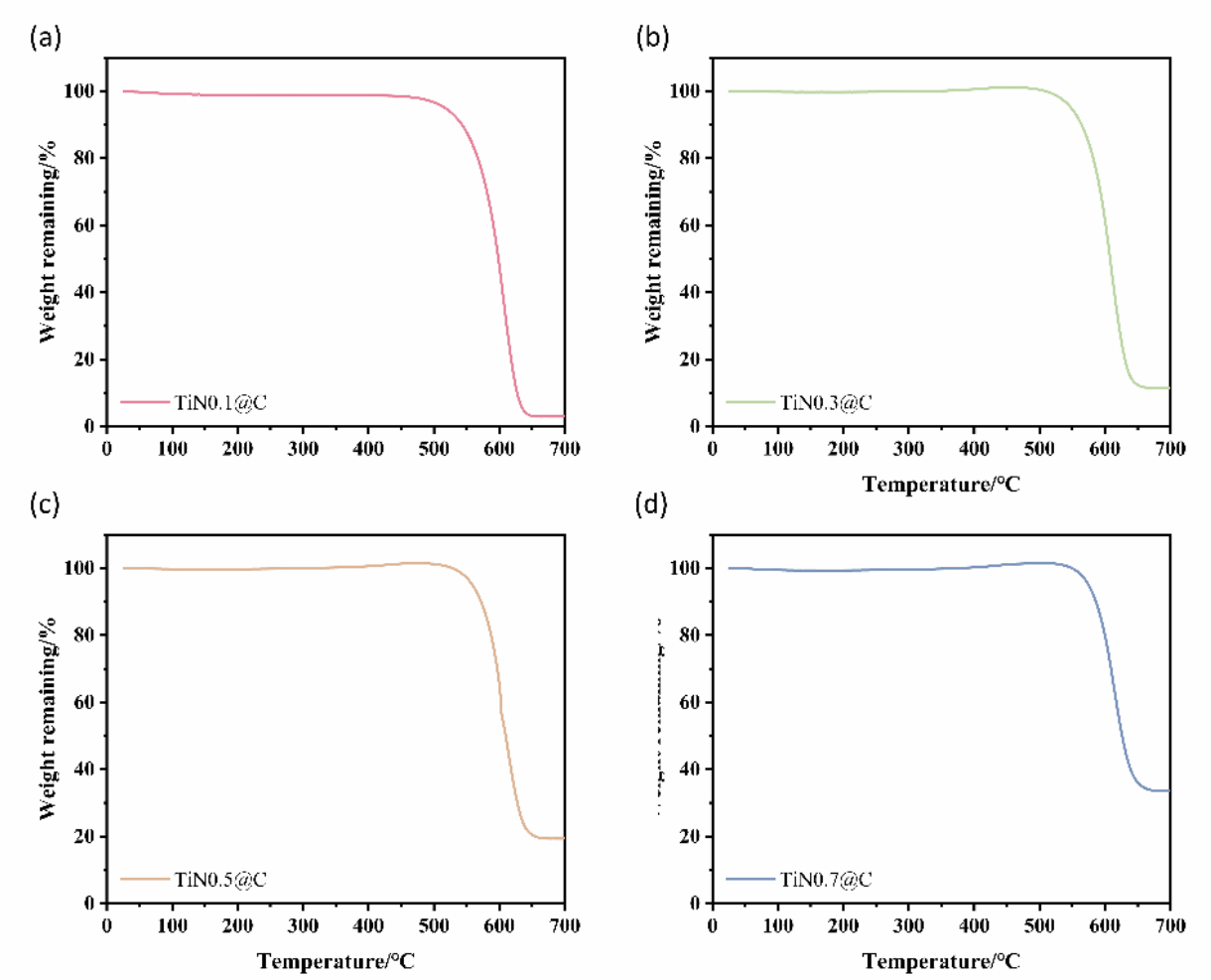

Fig. S2. TGA analysis of (a) 2.3 wt% TiN0.1@C; (b) 8.9 wt% TiN0.5@C; (c) 15.0 wt% TiN0.5@C and (d) 25.9 wt% TiN0.7@C under argon-oxygen mixture.

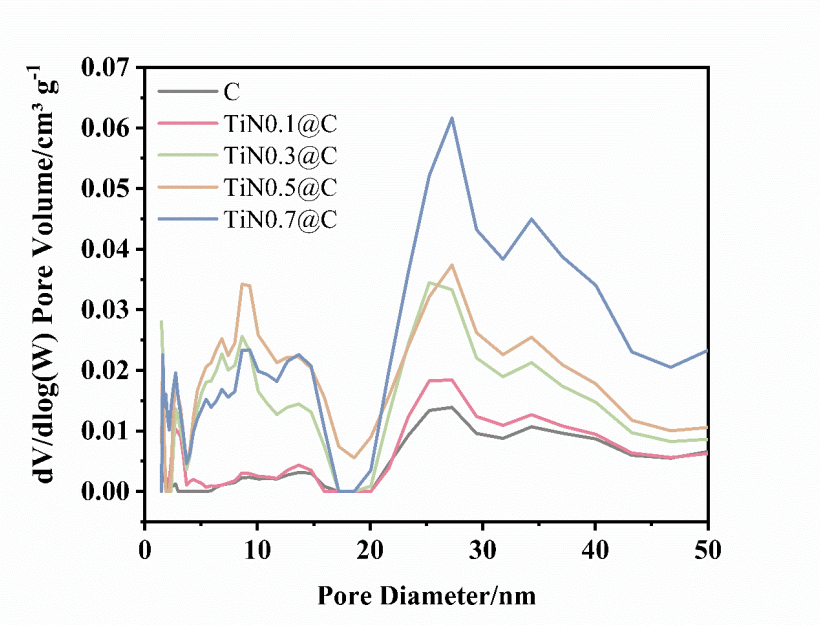

Fig. S3. Pore volume distribution of C, TiN0.1@C, TiN0.3@C, TiN0.5@C and TiN0.7@C. Data obtained using the non-local density functional theory (NLDFT) method.

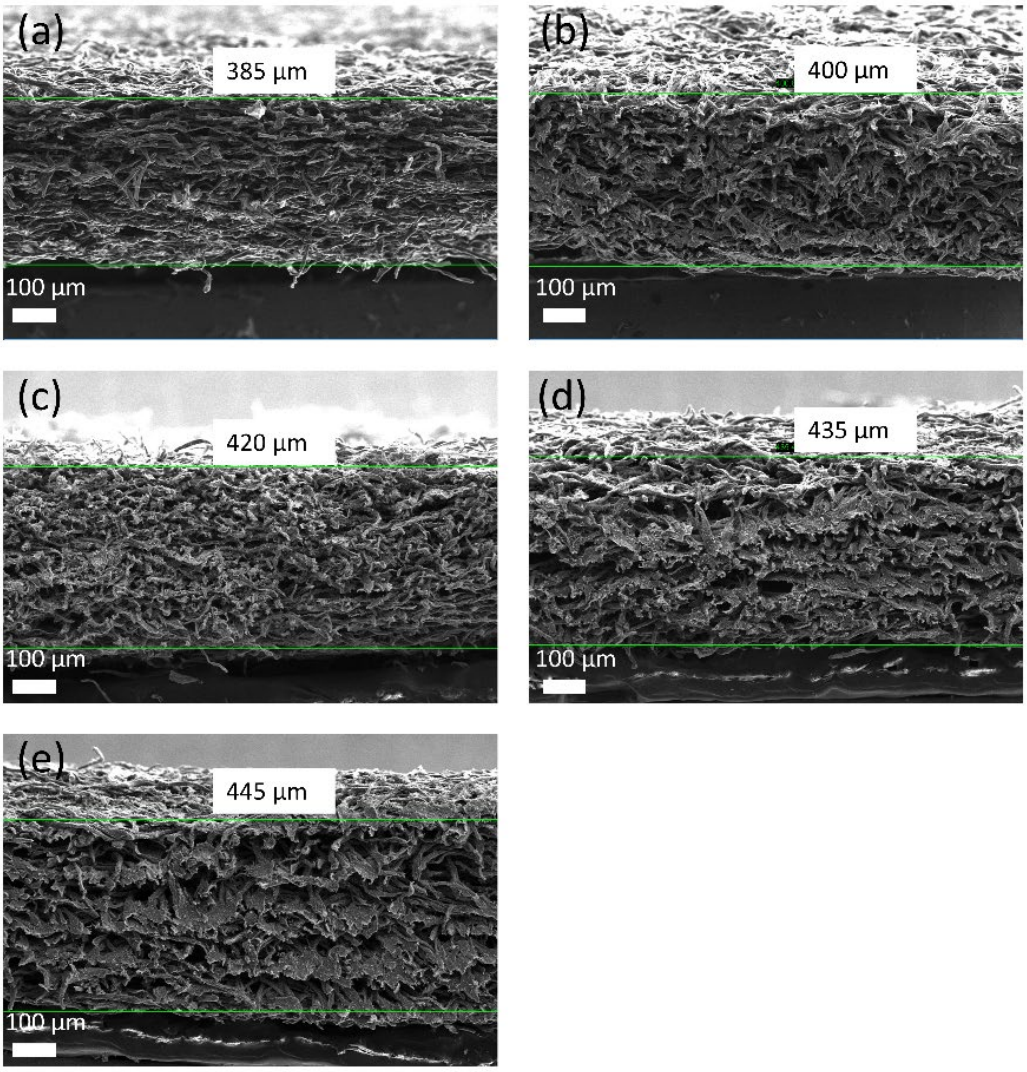

Fig. S4. Side-view SEM morphology of (a) C; (b) TiN0.1@C; (c) TiN0.3@C; (d) TiN0.5@C and (e) TiN0.7@C.

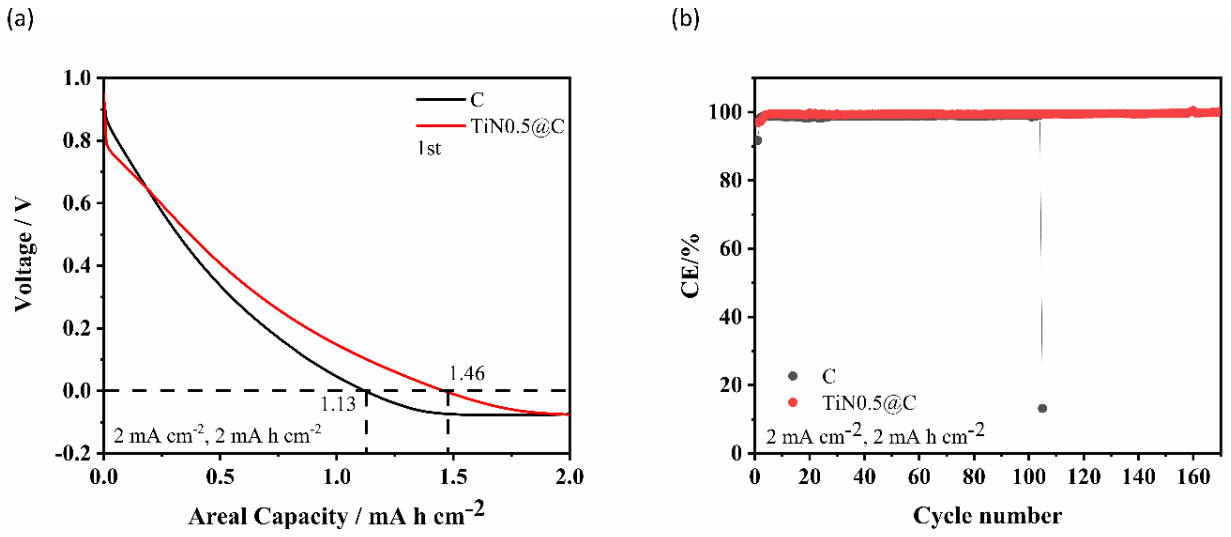

Fig. S5. (a) 1st cycle reduction curves of C or TiN0.5@C electrodes under a current density of 2 mA cm^{-2} with a lithium plating capacity of 2 mA h cm^{-2}; (b) CE of Li plating/stripping on C and TiN0.5@C at 2 mA cm^{-2} with a plating capacity of 2 mA h cm^{-2}.

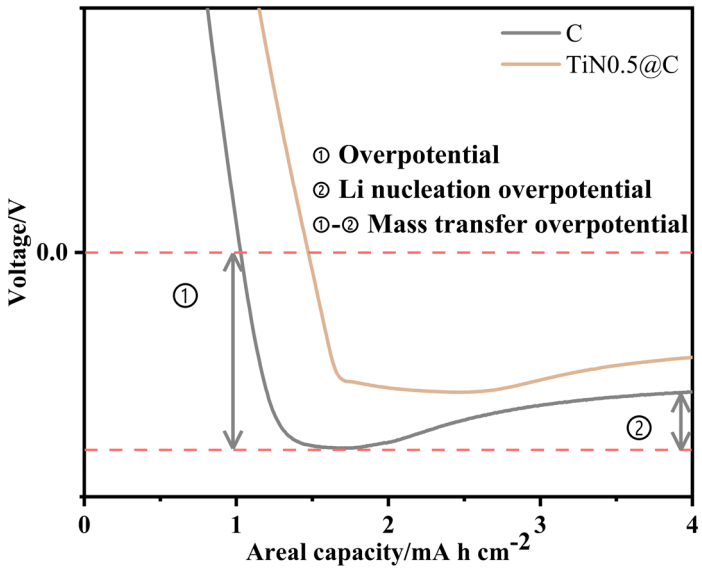

Fig. S6. Schematic illustration of different overpotential in the voltage profiles of C and TiN0.5@C.

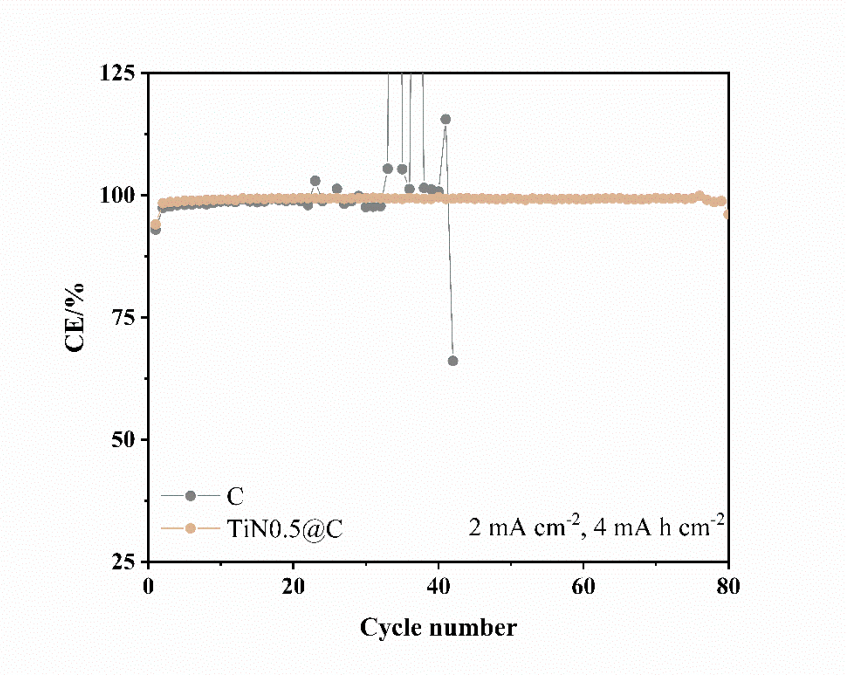

Fig. S7. CE of Li plating/stripping on C and TiN0.5@C at 4 mA cm^{-2} with a plating capacity of 4 mA h cm^{-2}.

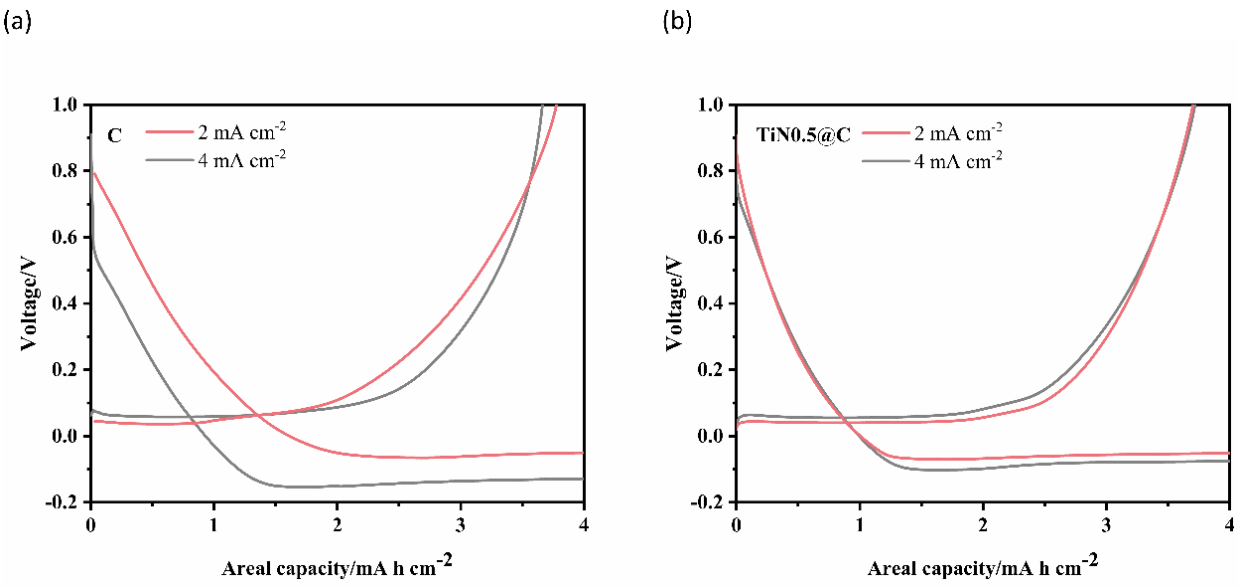

Fig. S8. Galvanostatic profiles for (a) C, (b) TiN0.5@C with a capacity of 4 mA h cm^{-2} at different areal current rates.

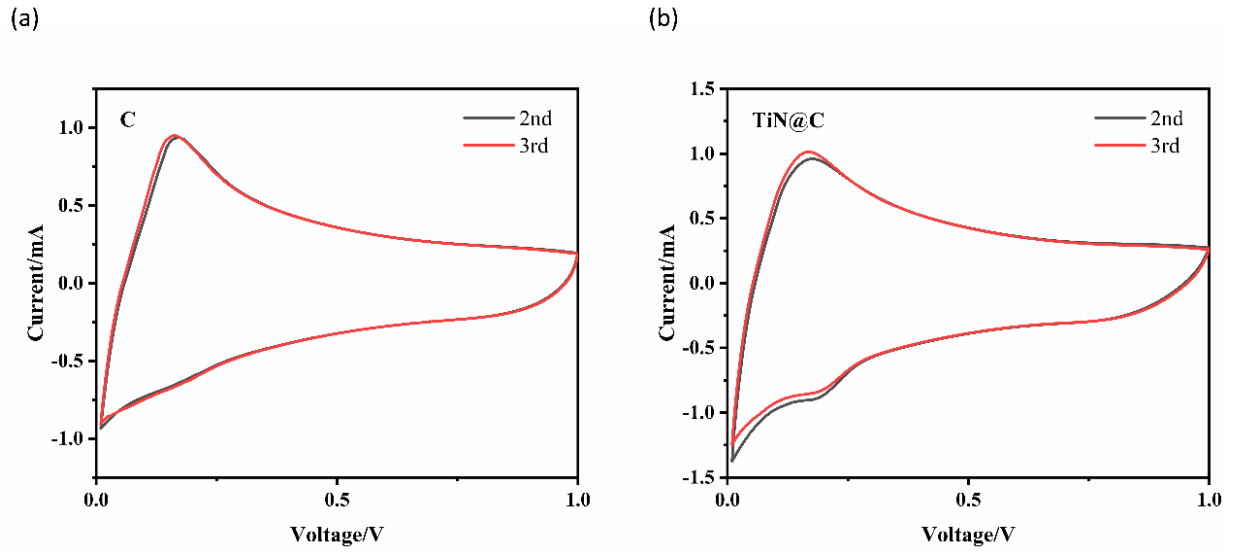

Fig. S9. (a) CV curves for the second and the third cycles of C and (b) TiN@C at the scan rate of 0.1 mV s^{-1}.

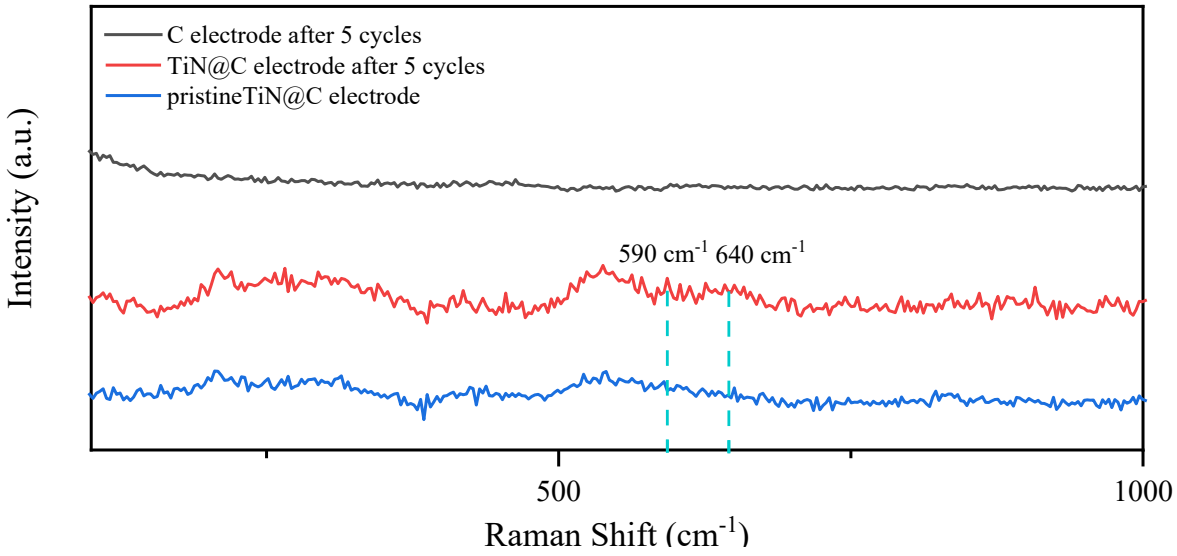

Fig. S10. Enlarged part of the Raman spectra of cycled C/cycled TiN@C/pristine TiN@C electrode in Figure 4k.

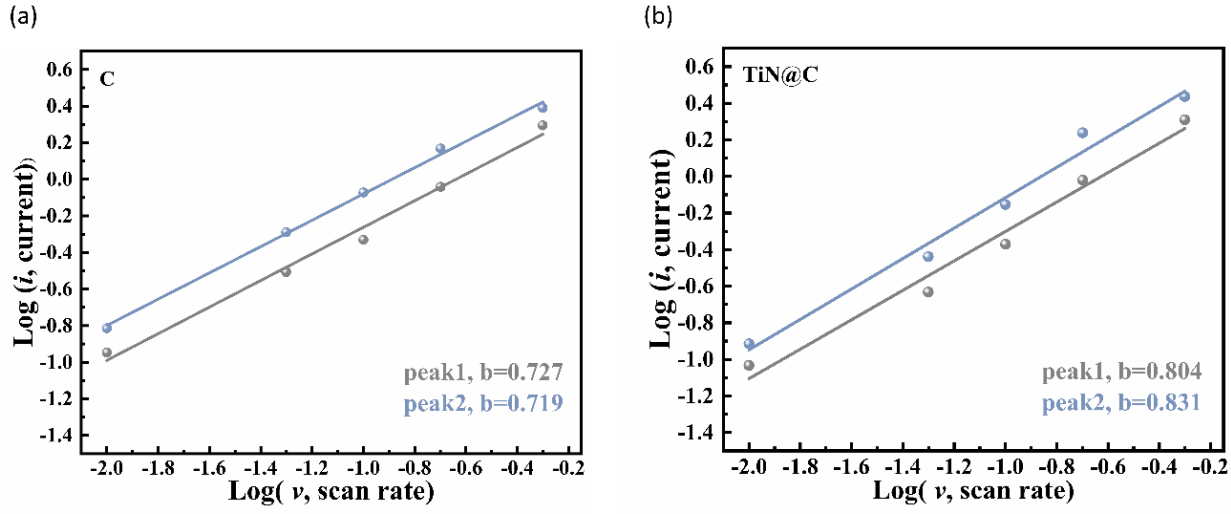

Fig. S11. b-value of (a) C and (b) TiN@C obtained by the log(i) versus log(v) plots at different oxidation and reduction peaks.

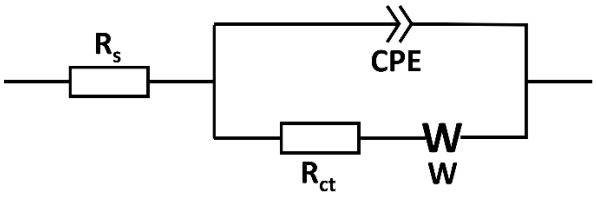

Fig. S12. EIS equivalent circuit diagram for Figure 5e.

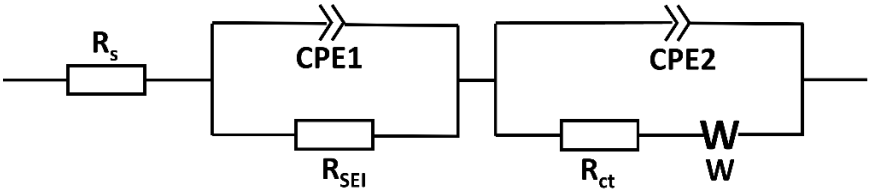

Fig. S13. EIS equivalent circuit diagram for Figure 5g and Figure S14.

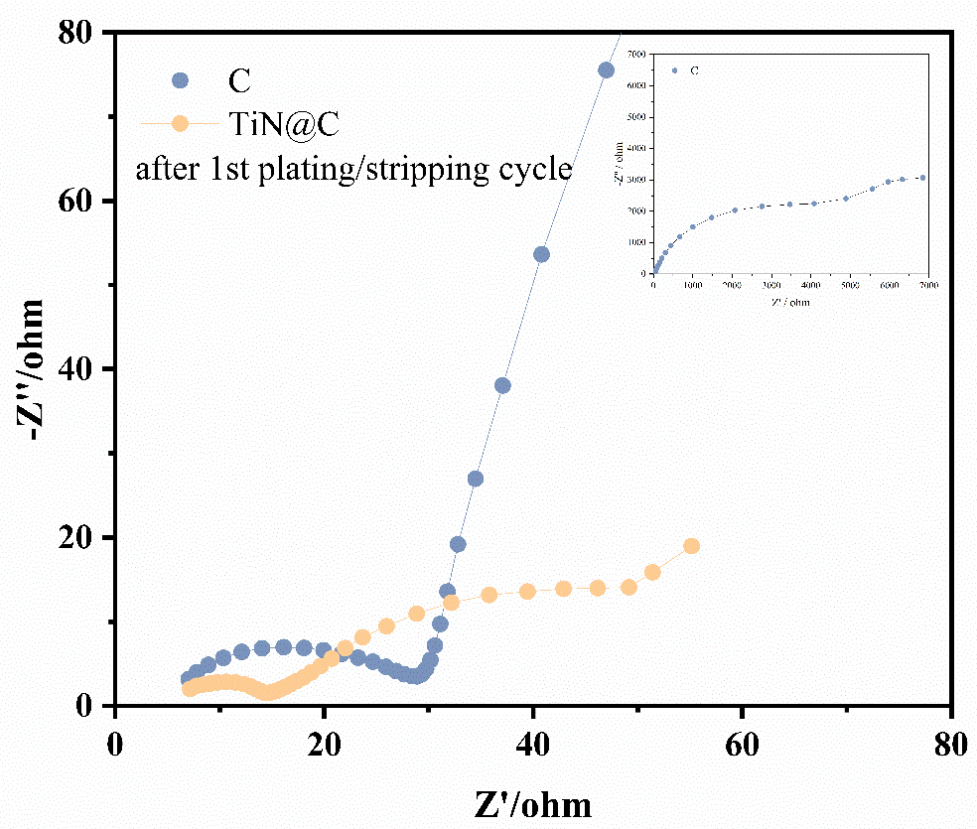

Fig. S14. Enlarged EIS part of bare C and TiN@C anodes after the 1st cycling (insert figure is the whole EIS pattern).

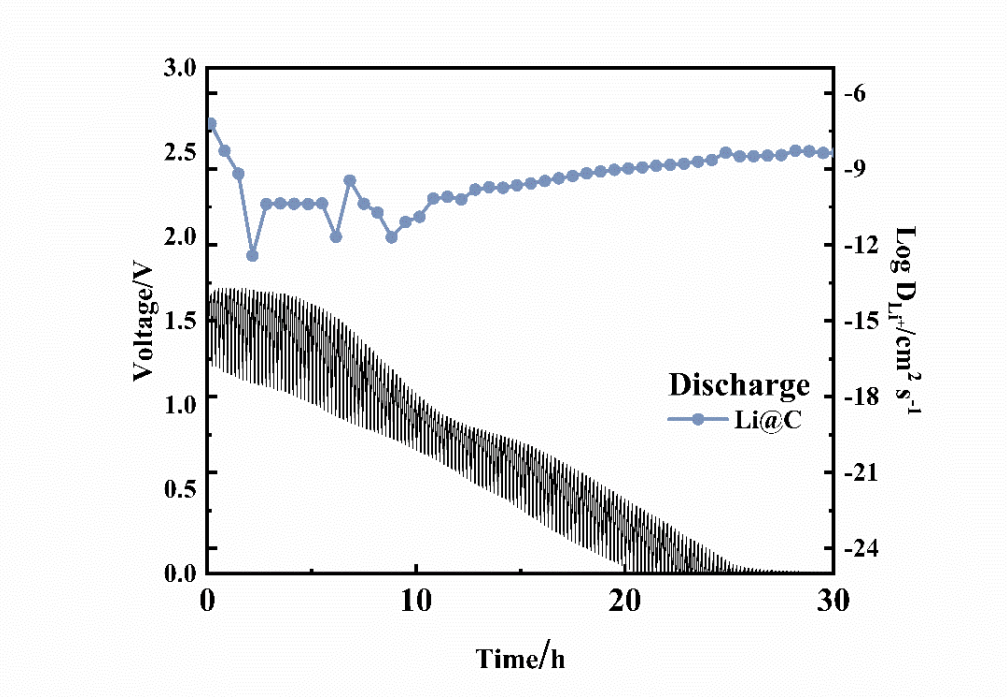

Fig. S15. GITT profile and the calculated Li^+ diffusion coefficients of Li@C electrode.

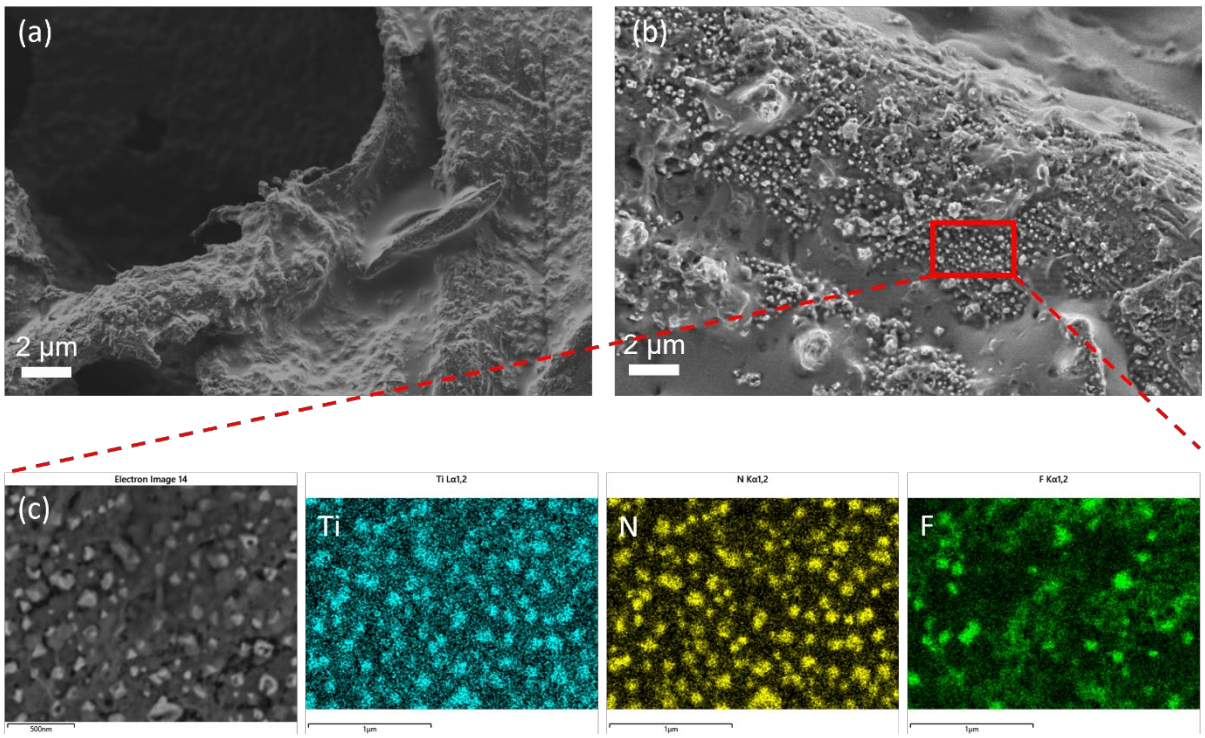

Fig. S16. SEM morphology of (a) C, (b) TiN@C electrodes after plating 2 mA h cm^{-2} Li; (c) Elemental mapping images for Ti, N, and F of selected TiN@C area.

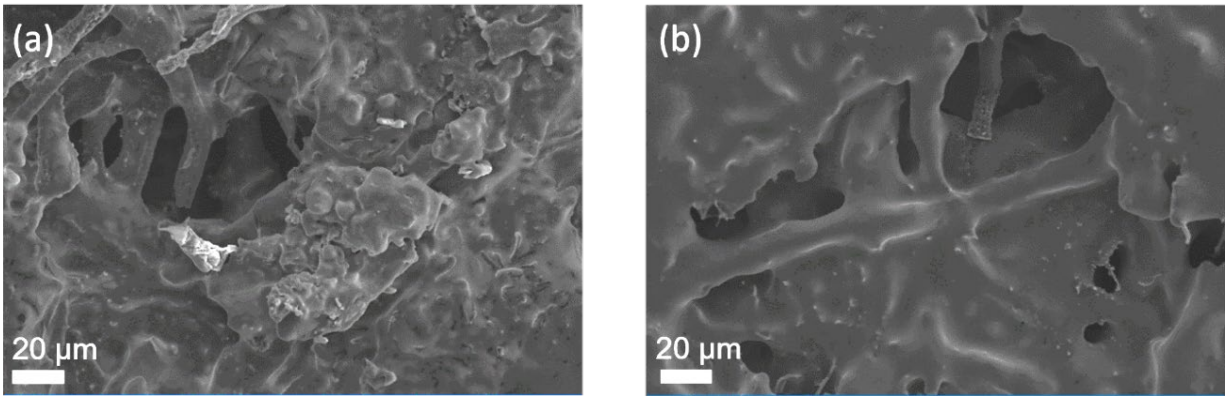

Fig. S17. SEM morphology of (a) C and (b) TiN@C after loading 8 mA h cm^{-2} Li.

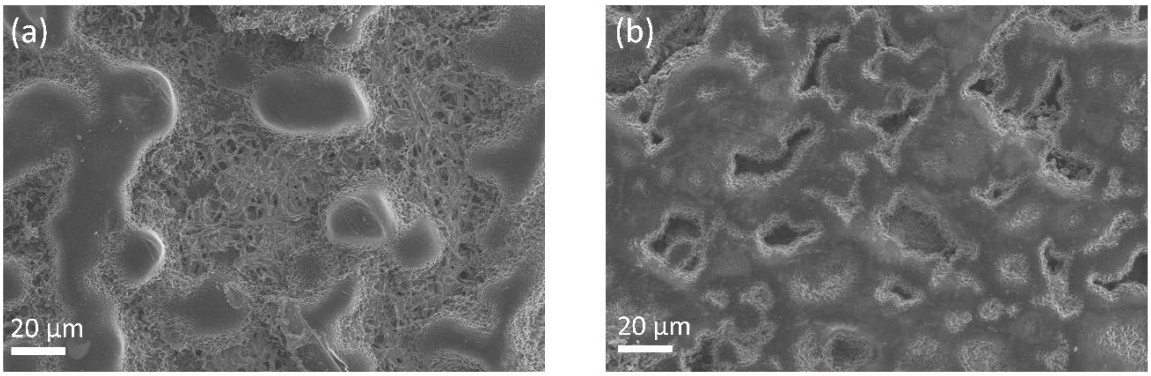

Fig. S18. SEM morphology of (a) C and (b) TiN@C after loading 20 mA h cm^{-2} Li.

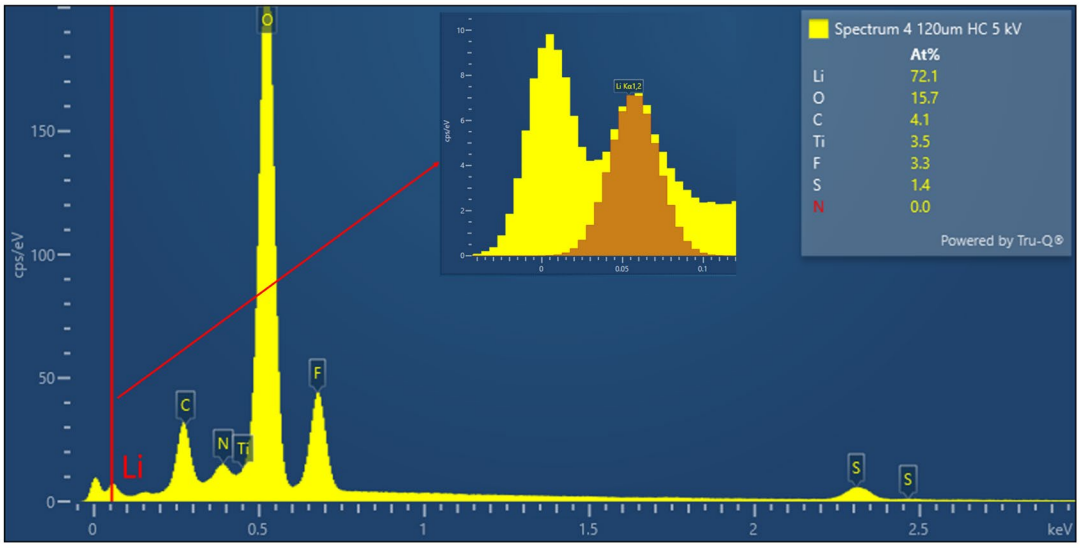

Fig. S19. EDS spectrum of TiN@C electrode after loading 20 mA h cm^{-2} Li (insert: zoomed of Li Ka peak with an expected fit match). Performed at 5 kV to maximise the lithium signal and balance the electron beam's interaction volume to the escape depth of the lithium X-rays.

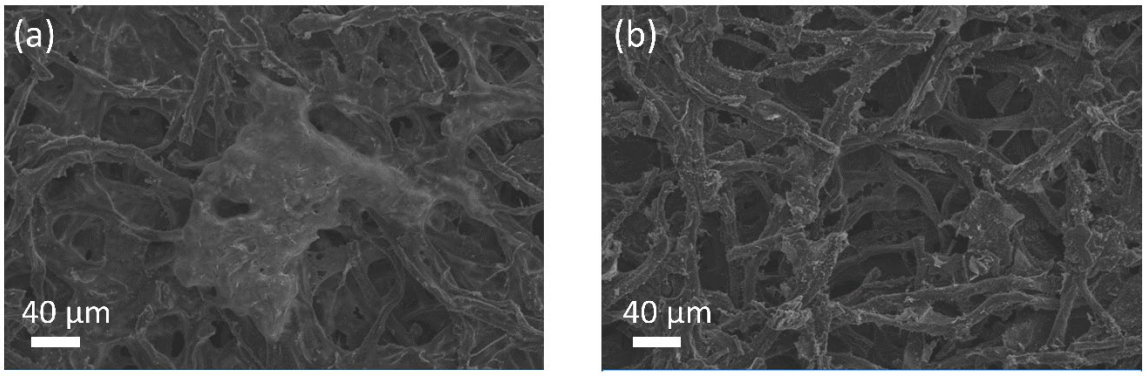

Fig. S20. SEM morphology of (a) C and (b) TiN@C after 100 cycles.

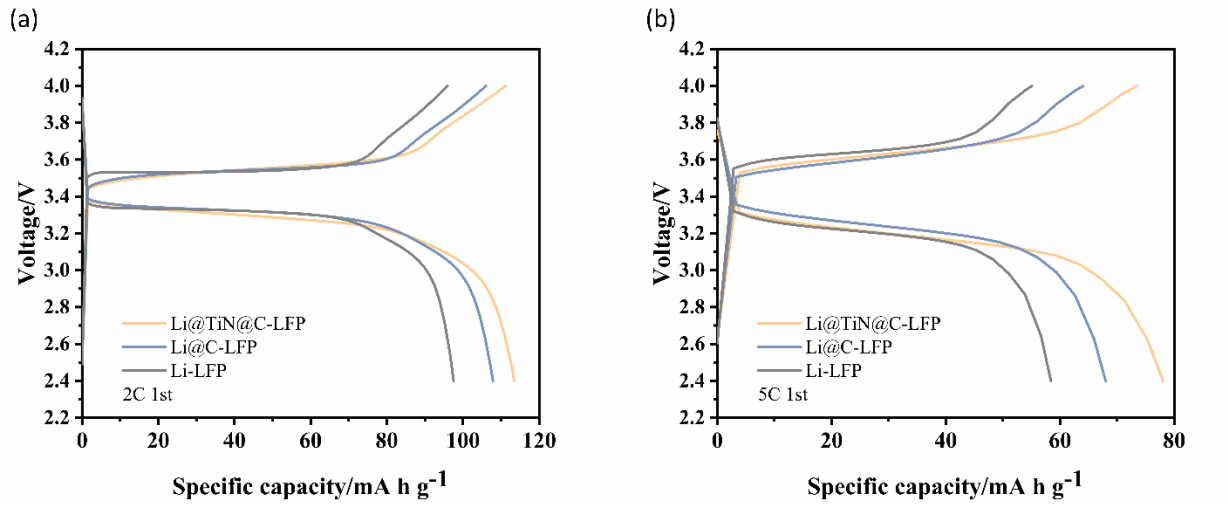

Fig. S21. The 1st charge-discharge profiles at (a) 2 C and (b) 5 C of Li@TiN@C-LFP, Li@C-LFP and Li-LFP cells.

Table S1. EIS results of C and TiN@C electrodes under different conditions.

Conditions	**Sample**	**R_s(Ω)**	**R_{ct}(Ω)**	**R_{SEI}(Ω)**	**W(Ω)**
Before cycling	C	9.95	159.50	-	3360.0
(After 20h rest)	TiN@C	4.09	149.10	-	496.2
After plating 6 mA h cm^{-2} Li	C	7.90	66.26	25.14	7.98
	TiN@C	7.31	58.21	14.21	5.17
After the 1st plating/stripping cycle	C	4.45	5181	24.35	18433
	TiN@C	5.5	17.87	8.34	48.43

Table S2. Nitride modifications of 3D lithium metal anodes

Substrate	Modification	Electrolyte	Half cells Conditions	Lifespan (cycles)	Symmetric cells Conditions	Lifespan (hours)	Ref
Cu foam	TiN	1 M LiTFSI in DOL/DME (1:1 vol%) with 2% $LiNO_3$	1 mA cm^{-2}, 1 mA h cm^{-2}	300	1 mA cm^{-2}, 1 mA h cm^{-2}	>900	[1]
Stainless steel mesh	CrN	1 M LiTFSI in DOL/DME (1:1 vol%) with 1% $LiNO_3$	1 mA cm^{-2}, 1 mA h cm^{-2}	400	1 mA cm^{-2}, 1 mA h cm^{-2}	2500	[2]
Ni foam	Ni_3N	1 M LiTFSI in DOL/DME (1:1 vol%) with 1% $LiNO_3$	1 mA cm^{-2}, 3 mA h cm^{-2}	300	2 mA cm^{-2}, 1 mA h cm^{-2}	300	[3]
Porous Ni structure	Ni_3N	1 M LiTFSI in DOL/DME (1:1 vol%) with 2% $LiNO_3$	1 mA cm^{-2}, 1 mA h cm^{-2}	300	2 mA cm^{-2}, 1 mA h cm^{-2}	1000	[4]
Carbon nanofibres	Mo_2N	1 M LiTFSI in DOL/DME (1:1 vol%) with 2% $LiNO_3$	1 mA cm^{-2}, 1 mA h cm^{-2}	150	3 mA cm^{-2}, 3 mA h cm^{-2}	1500	[5]
N doped rGO	Ni_3N	1 M LiTFSI in DOL/DME (1:1 vol%) with 2% $LiNO_3$	1 mA cm^{-2}, 1 mA h cm^{-2}	600	1 mA cm^{-2}, 1 mA h cm^{-2}	>1400	[6]
Carbon cloth	Fe_2N	-	1 mA cm^{-2}, 1 mA h cm^{-2}	400	1 mA cm^{-2}, 1 mA h cm^{-2}	1000	[7]
Carbon nanofibres	TiN	1 M LiTFSI in DOL/DME (1:1 vol%) with 1% $LiNO_3$	1 mA cm^{-2}, 1 mA h cm^{-2}	300	1 mA cm^{-2}, 1 mA h cm^{-2}	600	[8]
Carbon cloth	TiN nanorods	1 M $LiPF_6$ in EC/DEC (1 : 1) with 10 wt% FEC and 1 wt% VC	-	-	1 mA cm^{-2}, 1 mA h cm^{-2}	1000	[9]
Carbon paper	AlN nanoflake	1 M LiTFSI in DOL/DME with 1 wt% $LiNO_3$	1 mA cm^{-2}, 1 mA h cm^{-2}	350			[10]
Ni foam	g-C_3N_4	1 M LiTFSI in DOL/DME (1:1 vol%) with 1% $LiNO_3$	2 mA cm^{-2}, 1 mA h cm^{-2}	300	1 mA cm^{-2}, 1 mA h cm^{-2}	900	[11]
Carbon cloth	g-C_3N_4	1 M LiTFSI in DOL/DME (1:1	-	-	2 mA cm^{-2}, 10 mA h cm^{-2}	1500	[12]

		vol%) with 1% $LiNO_3$					
Graphene	g-C_3N_4	1 M LiTFSI in DOL/DME (1:1 vol%) with 1% $LiNO_3$	1 mA cm^{-2}, 1 mA h cm^{-2}	500	-	-	[13]
Layered and holey carbon	BN nanosheets	1 M LiTFSI in DOL/DME (1:1 vol%) with 2% $LiNO_3$	1 mA cm^{-2}, 1 mA h cm^{-2}	500	1 mA cm^{-2}, 1 mA h cm^{-2}	700	[14]
Carbon paper	TiN	1 M LiTFSI in DOL/DME (1:1 vol%) with 1% $LiNO_3$	2 mA cm^{-2}, 4 mA h cm^{-2}	200	0.5 mA cm^{-2}, 0.5 mA h cm^{-2}	1000	This work

1. Y. Wang, W. Zhang, Y. Qi, S. Wang, P. Liu, X. Wei, Y. Yu, W. Sun, X.-Z. Zhao and Y. Liu, *Journal of Alloys and Compounds*, 2021, **874**, 159916.
2. W. Hou, Y. Li, S. Li, Z. Liu, P. R. Galligan, M. Xu, J.-K. Kim, B. Yuan, R. Hu and Z. Luo, *Chemical Engineering Journal*, 2022, **441**, 136067.
3. J. Zhu, J. Chen, Y. Luo, S. Sun, L. Qin, H. Xu, P. Zhang, W. Zhang, W. Tian and Z. Sun, *Energy Storage Materials*, 2019, **23**, 539–546.
4. P. Qing, Z. Wu, Y. Chen, F. Tang, H. Yang and L. Chen, *Journal of Energy Chemistry*, 2022, **72**, 149–157.
5. L. Luo, J. Li, H. Yaghoobnejad Asl and A. Manthiram, *Advanced Materials*, 2019, **31**, 1904537.
6. L. Zhao, W. Wang, X. Zhao, Z. Hou, X. Fan, Y. Liu and Z. Quan, *ACS Applied Energy Materials*, 2019, **2**, 2692–2698.
7. Q. Chen, S. Chen, L. Zhao, J. Ma, H. Wang and J. Zhang, *Chemical Engineering Journal*, 2022, **431**, 133961.
8. K. Lin, X. Qin, M. Liu, X. Xu, G. Liang, J. Wu, F. Kang, G. Chen and B. Li, *Advanced Functional Materials*, 2019, **29**, 1903229.
9. S. Fang, L. Shen, S. Li, H. Dou and X. Zhang, *J. Mater. Chem. A*, 2020, **8**, 3293–3299.
10. C. Gao, B. Hong, K. Sun, H. Fan, K. Zhang, Z. Zhang and Y. Lai, *Energy Technology*, 2020, **8**, 1901463.
11. Z. Lu, Q. Liang, B. Wang, Y. Tao, Y. Zhao, W. Lv, D. Liu, C. Zhang, Z. Weng and J. Liang, *Advanced Energy Materials*, 2019, **9**, 1803186.
12. Y. Xu, T. Li, L. Wang and Y. Kang, *Advanced Materials*, 2019, **31**, 1901662.
13. P. Zhai, T. Wang, H. Jiang, J. Wan, Y. Wei, L. Wang, W. Liu, Q. Chen, W. Yang and Y. Cui, *Advanced Materials*, 2021, **33**, 2006247.
14. D. Cao, Q. Zhang, A. M. Hafez, Y. Jiao, Y. Ma, H. Li, Z. Cheng, C. Niu and H. Zhu, *Small Methods*, 2019, **3**, 1800539.